

Article

Study on the Relationship between Combustion Parameters and Cylinder Head Vibration Signal in Time Domain

Shaobo Ji ^{1,*}, Yang Li ¹, Guohong Tian ², Rongze Ma ¹, Minglei Shu ³ , Shiqiang Zhang ¹, Wenbin Yu ^{1,*}, Xin Lan ¹ and Yong Cheng ¹

¹ College of Energy and Power Engineering, Shandong University, Jinan 250061, China; 201934148@mail.sdu.edu.cn (Y.L.); 201914094@mail.sdu.edu.cn (R.M.); 202034543@mail.sdu.edu.cn (S.Z.); Lanxin@sdu.edu.cn (X.L.); cysgd@sdu.edu.cn (Y.C.)

² Department of Mechanical Engineering Sciences, University of Surrey, Guildford GU27XH, UK; g.tian@surrey.ac.uk

³ Shandong Computer Science Centre (National Supercomputer Centre in Jinan), Shandong Artificial Intelligence Institute, Qilu University of Technology (Shandong Academy of Sciences), Jinan 250013, China; shuml@sdas.org

* Correspondence: jobo@sdu.edu.cn (S.J.); wbyu@sdu.edu.cn (W.Y.)

Abstract: Combustion-related characteristic parameters, such as the start of combustion (SoC) and the timing of the peak pressure increase rate (PIR), can be used as the feedback signals for the closed-loop control of combustion. A dynamic Finite Element Method (FEM) model was firstly developed to confirm the closely related time period between combustion pressure and vibration. On this basis, a fast processing method was developed to estimate the timings of SoC and the peak PIR in the closely related time period. This method was verified on a twelve-cylinder heavy-duty diesel engine at various engine speed and load. Results showed that the maximum deviation of the two parameters were within 2 °CA and 1.5 °CA, respectively, which suggested that the proposed method had an adequate accuracy.

Keywords: combustion pressure; vibration signal; FEM analysis; combustion information estimation



Citation: Ji, S.; Li, Y.; Tian, G.; Ma, R.; Shu, M.; Zhang, S.; Yu, W.; Lan, X.; Cheng, Y. Study on the Relationship between Combustion Parameters and Cylinder Head Vibration Signal in Time Domain. *Energies* **2021**, *14*, 6421. <https://doi.org/10.3390/en14196421>

Academic Editor: Andrzej Teodorczyk

Received: 9 September 2021

Accepted: 2 October 2021

Published: 8 October 2021

Publisher's Note: MDPI stays neutral with regard to jurisdictional claims in published maps and institutional affiliations.



Copyright: © 2021 by the authors. Licensee MDPI, Basel, Switzerland. This article is an open access article distributed under the terms and conditions of the Creative Commons Attribution (CC BY) license (<https://creativecommons.org/licenses/by/4.0/>).

1. Introduction

It is essential to measure and control the combustion process of internal combustion engines (ICE) to meet increasingly stringent emissions and fuel economy requirements [1,2]. In-cylinder pressure history contains a wealth of useful information of combustion process, such as peak pressure and PIR, and their locations. Combustion pressure can be obtained directly by pressure transducers mounted on the cylinder head using an intrusive method. The pressure transducers are expensive and fragile, thus not suitable for long-term and continuous monitoring due to the harsh environment they operate in [3]. Abrupt pressure rise caused by the combustion process results in gas oscillation in the combustion chamber, which leads to an excitation force that produces the vibration and noise of an engine [4,5]. The vibration signal contains abundant combustion information and has been an attractive idea due to low cost and convenience of installation. The vibration signal has been used for knock detection with different signal processing method, such as fast Fourier transform (FFT), Empirical Mode Decomposition (EMD), Discrete Wavelet Transform, and time-frequency method [6–9]. The vibration signal was also used to detect misfire fault by decision tree algorithm [10] and multi-net neural network system [11].

Considering the important role of combustion pressure on combustion status analysis, some researchers conducted studies to reconstruct the combustion pressure according to the vibration signal. Bizon et al. [12] measured vibration signal from a three-cylinder diesel engine with an accelerometer and established a radial basis function (RBF) network with the vibration signal as input to predict the cylinder pressure. The result showed that it was

feasible to reconstruct combustion pressure from the vibration signal. Johnsson et al. [13] reconstructed the cylinder pressure of a six-cylinder ethanol engine with vibration signal and crankshaft speed as input. The accuracy was verified by comparing the combustion pressure obtained from the reconstruction and measurement. Bizon et al. [14] established a RBF network to train and reconstruct the combustion pressure of a one cylinder diesel engine according to the vibration signal. The angular locations of peak pressure and 50% mass fraction burned (MFB50) from the reconstructed and measured combustion pressure were compared, and results showed that the deviations of the two angular locations were lower than 1° CA. Except for the Artificial Neural Network method, Ghamry et al. [15] reconstructed cylinder pressure according to the cepstrum analysis of acoustic emission produced by engine vibration.

The vibration signal was also used to estimate combustion information directly according to the correlation between the two signals. Omar et al. [16] calculated the root-mean-square (RMS) value of vibration signal measured from the cylinder block, which was used to reflect the combustion status of engines running with different kinds of fuel. Scafati et al. [17] measured the vibration acceleration from a four cylinders diesel engine and compared with the cylinder pressure. The comparison result showed that the MFB50 can be estimated from the filtered vibration acceleration. Chiatti et al. [18] calculated the coherence function between the vibration acceleration and the combustion pressure obtained from a two cylinders engine, and the result showed that the vibration acceleration under 2 kHz can be used to estimate the MFB50. Carlucci et al. [19] analyzed the relationship between the vibration measured from cylinder block and heat release rate (HRR). Results showed that the amplitude of vibration signal was closely related with the HRR. Morello et al. [20] measured the vibration signal from a six-cylinder diesel engine and then filtered with different windowing functions. The relationship between the filtered signal and HRR was analyzed. A similar study was conducted by Lee et al. [21], and the results showed that the integrated value of vibration in the frequency band from 300 to 1500 Hz was proportional to the peak HRR.

Except for the MFB50 and HRR, other combustion parameters, such as the appearance timing of peak pressure and the peak PIR, also contain useful information of combustion and can be used for the closed-loop control of the ICE. Zhao et al. [22] measured vibration acceleration signal from a one-cylinder diesel engine and then reconstructed with the EMD method. The reconstructed signal was used to estimate the appearance timing of the peak pressure. Zhao et al. [23] established an analysis model to remove the interface from measured vibration velocity signal. The treated signal was then used to estimate the location of peak pressure and PIR for a one-cylinder diesel engine.

The above-mentioned studies were mainly conducted by spectrum analysis, and the results confirmed the correlation between the combustion characteristics and spectrum component of vibration. The vibration signals also contain abundant information of combustion process in time domain. Considering the periodic operation pattern of ICEs, there exists a closely related time period between combustion pressure and vibration. The vibration signals in this time period have a potential to be more suitable to estimate combustion characteristics with less requirement of computational resources. However, there were few studies to investigate the time domain correlation, and the closely related time period still requires more in-depth study. In addition, most of the existing vibration signal processing methods were complicated and struggled to meet the real-time request of closed-loop control.

This paper aimed to bridge the knowledge gap by proposing a fast processing method to estimate the combustion parameters in real time with an adequate accuracy. The main research flow chart was shown in Figure 1. Due to the complexity of an engine structure, a FEM model of one-cylinder engine was firstly developed to investigate the time correlation between the vibration signals and combustion parameters. Analysis results of the model indicated that vibration signal showed a two-stage feature. On this basis, the closely related time period between combustion pressure and vibration was confirmed. The

vibration acceleration and PIR were compared, and a fast processing method to estimate the timings of SoC and the peak PIR was demonstrated. The method was finally verified on a twelve-cylinder heavy-duty diesel engine, which showed a satisfactory accuracy.

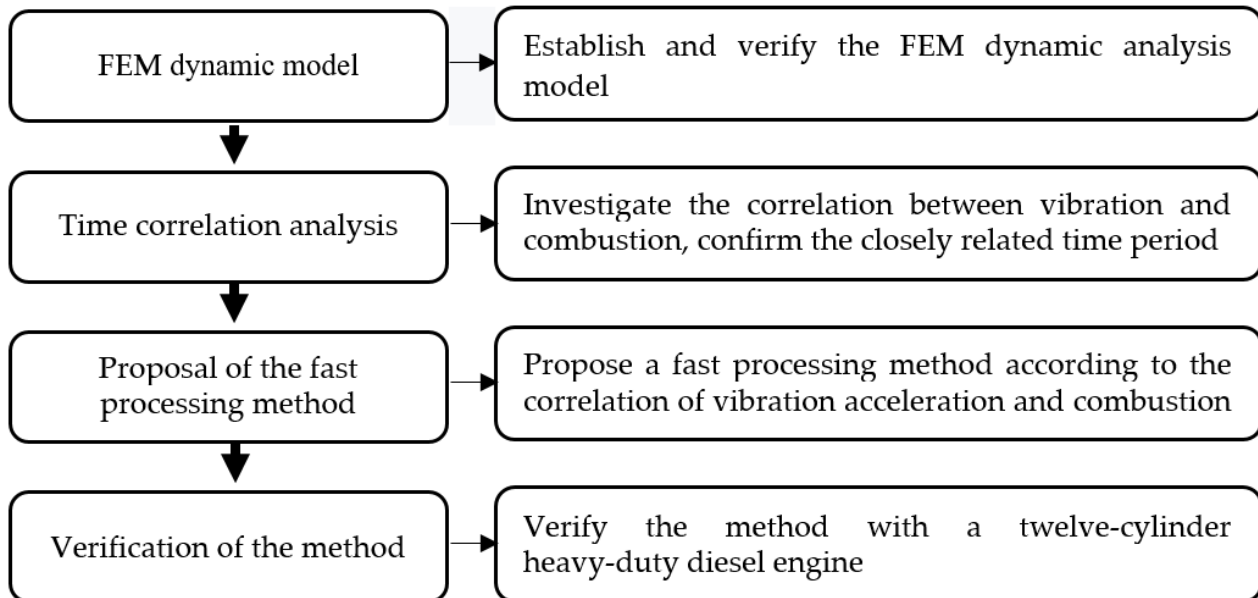


Figure 1. The main research flow chart.

2. Experimental Setup and Finite Element Analysis Model

2.1. Experimental Setup

The experiments were conducted with a twelve-cylinder diesel engine. Table 1 shows specifications of the engine, and Figure 2 shows the schematic illustration of the test bench. The engine was coupled to a dynamometer to control the engine speed and load during the experiments. The measurement accuracy of the engine speed and torque were $\pm 1\%$ and $\pm 0.5\%$, respectively. A piezoelectric transducer (12QP250) was used to measure the combustion pressure of the third cylinder for the twelve-cylinder engine. The output of the piezoelectric transducer was amplified with a charge amplifier (YE5850A) with the precision of 1%. A vibration accelerometer (CA-YD-102) was bolted on the third cylinder head with the same direction as the axis of the cylinder. The output of the accelerometer was amplified with a charge amplifier (YE5852A) with the precision of 1%. A data acquisition card (MP426) with 16-bit resolution was used to sample the cylinder pressure, accelerometer signal, and crank phase signal simultaneously with the sampling frequency of 50 kHz per channel. Table 2 shows the detailed specifications of the sensors.

Table 1. Specifications of the engines.

Engine Type	Twelve Cylinders Engine
Description	V-type, four valves, turbocharged, Electronic unit pump
Cylinder bore \times stroke (mm \times mm)	190 \times 210
Displacement (L)	71.4
Compression ratio	14:1
Rated speed (rpm)	1300
Max. power (kW)	1000@1300 rpm
I/O / IVC ($^{\circ}$ CA)	24 $^{\circ}$ CA BTDC / 28 $^{\circ}$ CA ABDC
EVO / EVC ($^{\circ}$ CA)	28 $^{\circ}$ CA BBDC / 24 $^{\circ}$ CA ATDC

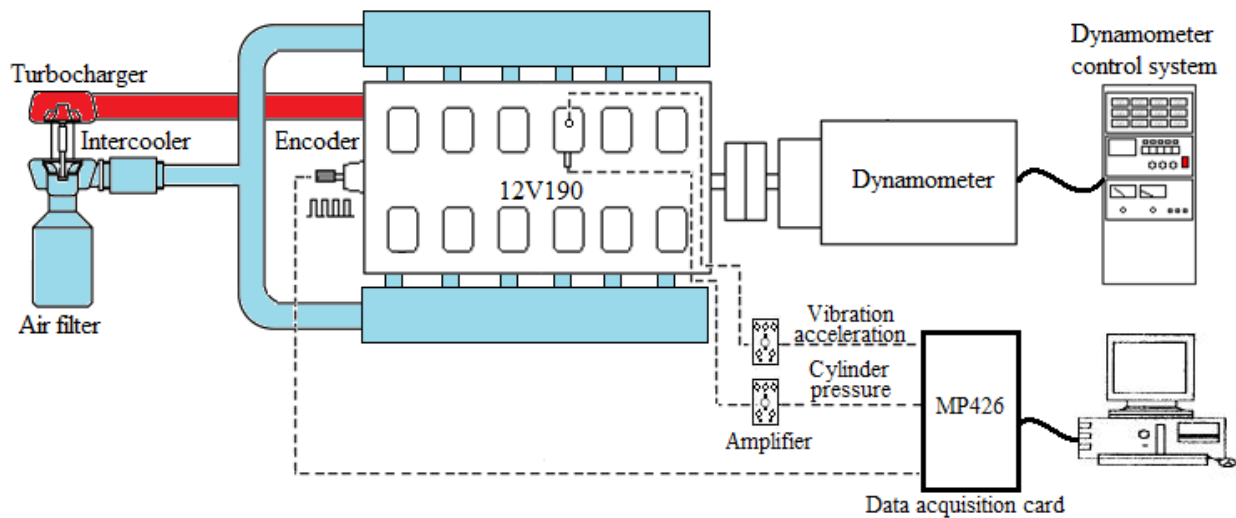


Figure 2. The schematic illustration of the test bench.

Table 2. Specifications of pressure transducer and accelerometer.

Sensor	12QP250	CA-YD-102
Range	0–15 MPa	0–5000 g
Resonant frequency	75 kHz	40 kHz
Sensitivity	200 pC/MPa	0.7 pC/g

The experiment of the twelve-cylinder engine was used to verify the precision of the combustion parameter estimation. In the experiment, the operation conditions, such as engine torque (T_{tq}) and speed (n), were adjusted, which is shown in Table 3. All experiments were conducted when the engines were running at steady states, with oil and water temperature maintained at 85°C and 80°C, respectively.

Table 3. Operation conditions for twelve-cylinder engine.

Engine Speed (rpm)	Engine Power (kW)
1200	100, 200, 300, 400
1500	150, 300, 450, 675, 880, 1000

2.2. Finite Element Analysis Model

Considering the complex structure of ICEs, three-dimensional modelling is a better choice to reflect the structural feature and transfer characteristics of the ICEs. Finite Element Analysis has been used to optimize the vibration-acoustic performance [24] and component failure analysis of ICEs, such as connecting rods [25], crankshafts [26], and so on. The above studies were mainly conducted with static finite element analysis method. In this study, a dynamic FEA model of a one-cylinder diesel engine was established with ABAQUS software, which has a high-performance in dynamic response analysis. The dynamic analysis equation of the FEA model can be expressed as Equation (1):

$$[M]\{\ddot{q}\} + [D]\{\dot{q}\} + [K]\{q\} = \{R(\dot{q}, q, t)\} \quad (1)$$

where, $[M]$, $[D]$, and $[K]$ are the mass, damping, and stiffness matrices of the system. $\{\ddot{q}\}$, $\{\dot{q}\}$, and $\{q\}$ are the acceleration, velocity, and displacement, respectively. $\{R(\dot{q}, q, t)\}$ is the load of the system.

The model was composed of a cylinder head and a block. The water tank and the cylinder head cover that existed in the real engine were neglected, considering their small impact on the FEA model. To ensure the calculation accuracy, the main structure, such

as water jacket, intake port, and stiffener and so on were retained in the model. Some micro-structure, such as chamfering, was neglected to reduce the complexity of the model. The simplified three-dimensional model was imported to ABAQUS and generated mesh model according to the comprehensive consideration of accuracy and calculation time. Figure 3a showed the mesh model, which was consisted of 19,694 nodes and 63,302 four-node tetrahedron elements. The material of cylinder head and block was HT250 with the density, Poisson's ratio, and elastic modulus of 7200 kg/m^3 , 0.27, and 113,000 MPa, respectively. In the experiment, the engine was bolted by four brackets, so the freedoms of the fixed points were fully constrained in the FEA model, which is shown in Figure 3b. The dynamic FEA was calculated with the Full Newton method. The procedure type of the Step used was Dynamic and Implicit.

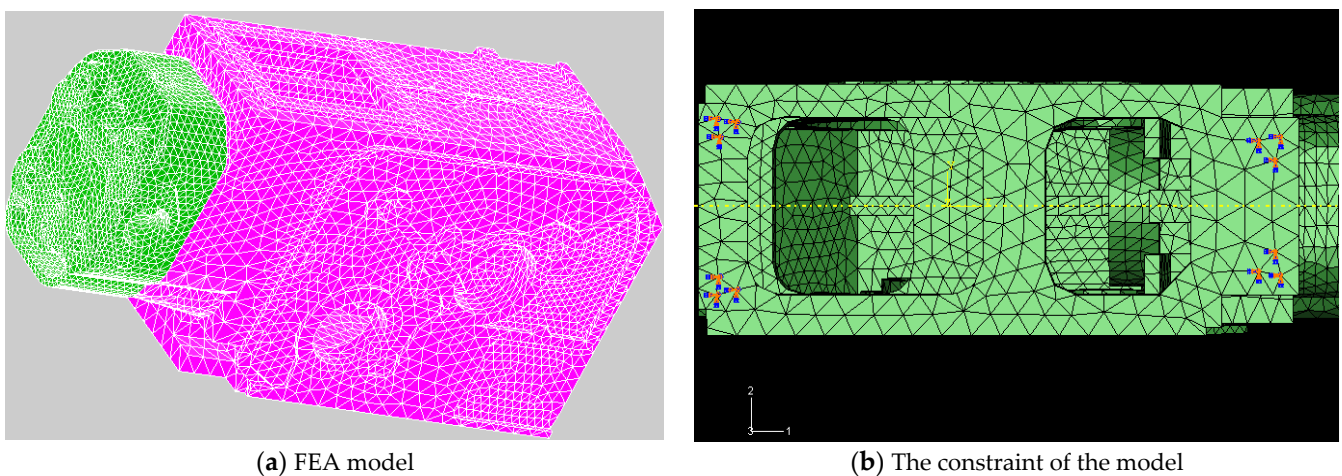


Figure 3. The model and constraint of the one-cylinder engine.

The simulation was conducted to analyze the relationship between combustion excitation and the corresponding vibration signals. In order to conduct single-parameter analysis, combustion pressure was the only excitation source, and other excitations, such as the piston slap-induced forces, valve seating forces, and crankshaft rotation-induced forces, were neglected in the model. The combustion pressure was measured in different working conditions. The combustion in the cylinder was considered a quasi-equilibrium process, and the main effect was to produce a downward thrust on the piston and an upward thrust to the fire-face of the cylinder head during the power stroke. The measured combustion pressure was exerted on the fire-face of the cylinder head evenly, as shown in Figure 4. The force on the cylinder wall was cancelled out in all directions and therefore neglected.

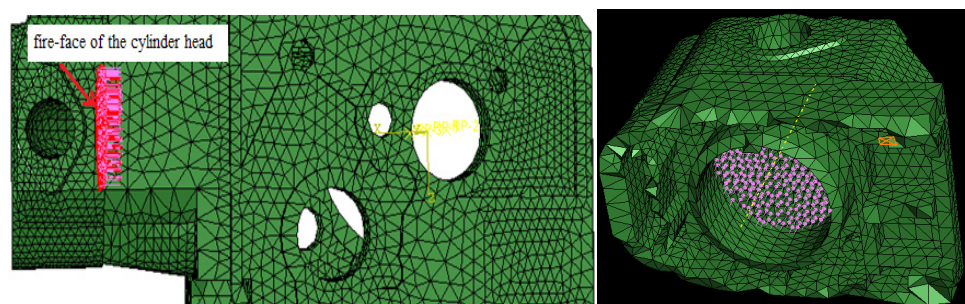


Figure 4. Application of combustion pressure in the FEA model.

The dynamic FEA model was validated by comparing the calculated and measured acceleration. Figure 5 showed the comparison under the load of 20 N·m and the speed of 1200 rpm. There existed certain differences in the amplitude and phase of the two results.

The difference was mainly attributed to the application's deviation of constraint and load. In addition, the measured acceleration contained response signals of other excitations, while the acceleration from the dynamic FEA model mainly contained the response of combustion. In general, the trend between the measured and calculated result was similar.

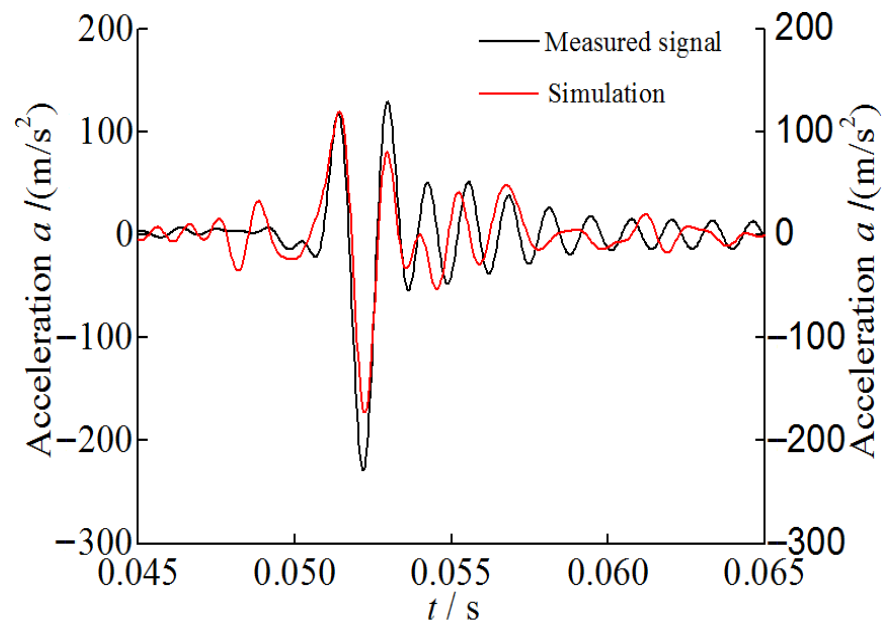


Figure 5. Comparison of acceleration between measurement and simulation.

To verify the dynamic FEA model furtherly, the vibration displacement of the cylinder head was calculated based on the FEA model. According to the relationship between vibration acceleration and displacement, the Simpson integral algorithm was employed to obtain the vibration displacement according to the measured vibration acceleration [27]. The two vibration displacements were compared in Figure 6, and it can be seen that the two signals had the similar trend before the peak vibration, and after that, the two signals presented fluctuation. The reason for the fluctuation was explained in the following sections. The comparison of the vibration displacements in the time domain also showed that the dynamic FEA model can be used to study the correlation between the combustion excitation and the corresponding vibration response.

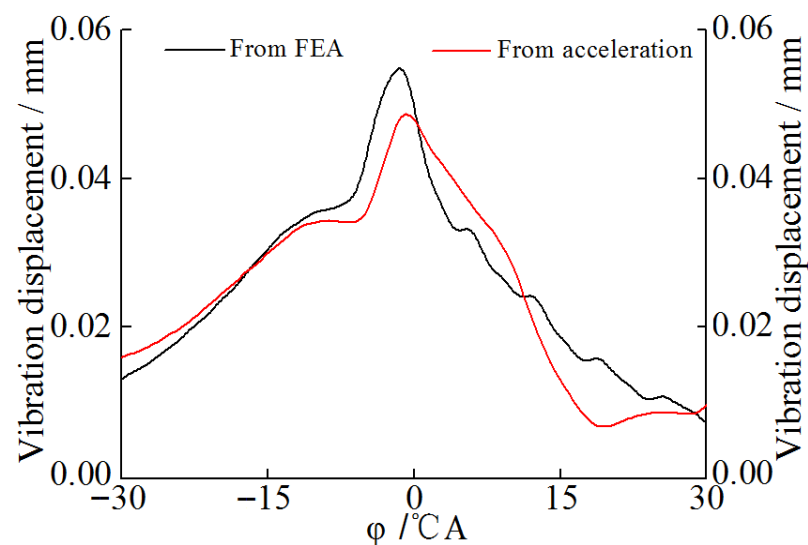


Figure 6. Comparison of the vibration displacement.

3. Results and Discussion

3.1. FEA Analysis

The dynamic FEA model was firstly used to investigate the transfer characteristic of the engine. An ICE can be considered as a test system in which the combustion pressure is an input, and the vibration signal is an output. To understand the performance of the test system, the amplitude-frequency characteristic was calculated using the dynamic FEA model. The vibration displacement of the cylinder head was calculated, and the amplitude ratio of vibration is shown in Figure 7. It can be seen that the engine was a typical multiple-degree-of-freedom (MDOF) system, and there existed three natural frequencies, which were approximately 620, 740, and 1200 Hz under the frequency of 2000 Hz. When the excitation frequency was lower than 500 Hz, the amplitude ratio was about 1, which meant that the excitation and response were linearly related. The amplitude ratio was higher than 1 around the natural frequency, which indicated that the relationship between the excitation and response was affected by the transfer characteristic of the engine in these frequency ranges.

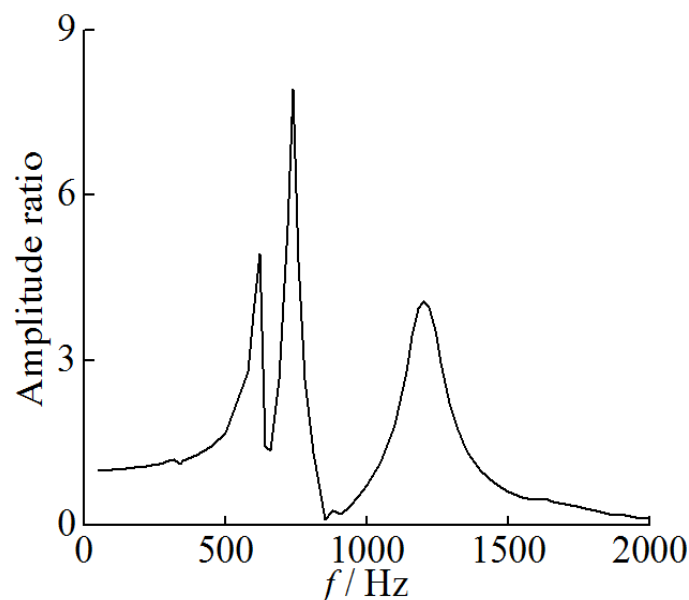


Figure 7. The calculation result of the amplitude-frequency characteristic.

Experiments were conducted when the one-cylinder engine was driven by a motor and operated normally at the load of 40 N·m and the speed of 1200 rpm. The measured cylinder pressure was exerted to the dynamic FEA model. Calculated vibration displacement was compared with the pressure, which is shown in Figure 8a,b. The trend of the pressure and vibration displacement was similar when the engine was driven by a motor. When the engine was operated normally, the relationship between the two signals can be divided into two stages by appearance timing of the peak pressure. Before the appearance timing of the peak pressure, the two signals had a similar trend, and after that, the calculated displacement presented an obvious fluctuation. To explain the phenomenon, the frequency spectrum of the cylinder pressure was calculated by the FFT method, and the result is shown in Figure 8c. When the engine was driven by a motor, the spectrum energy of the pressure was mainly concentrated in the low-frequency band, which was mainly smaller than 300 Hz. The amplitude ratio was about 1 in this frequency range, which led to the similar trend of the pressure and vibration displacement. When the engine was operated normally, some frequency components of pressure were already higher than the first-order natural frequency. The transfer characteristic of the engine was contributed to the difference between the combustion pressure and vibration displacement.

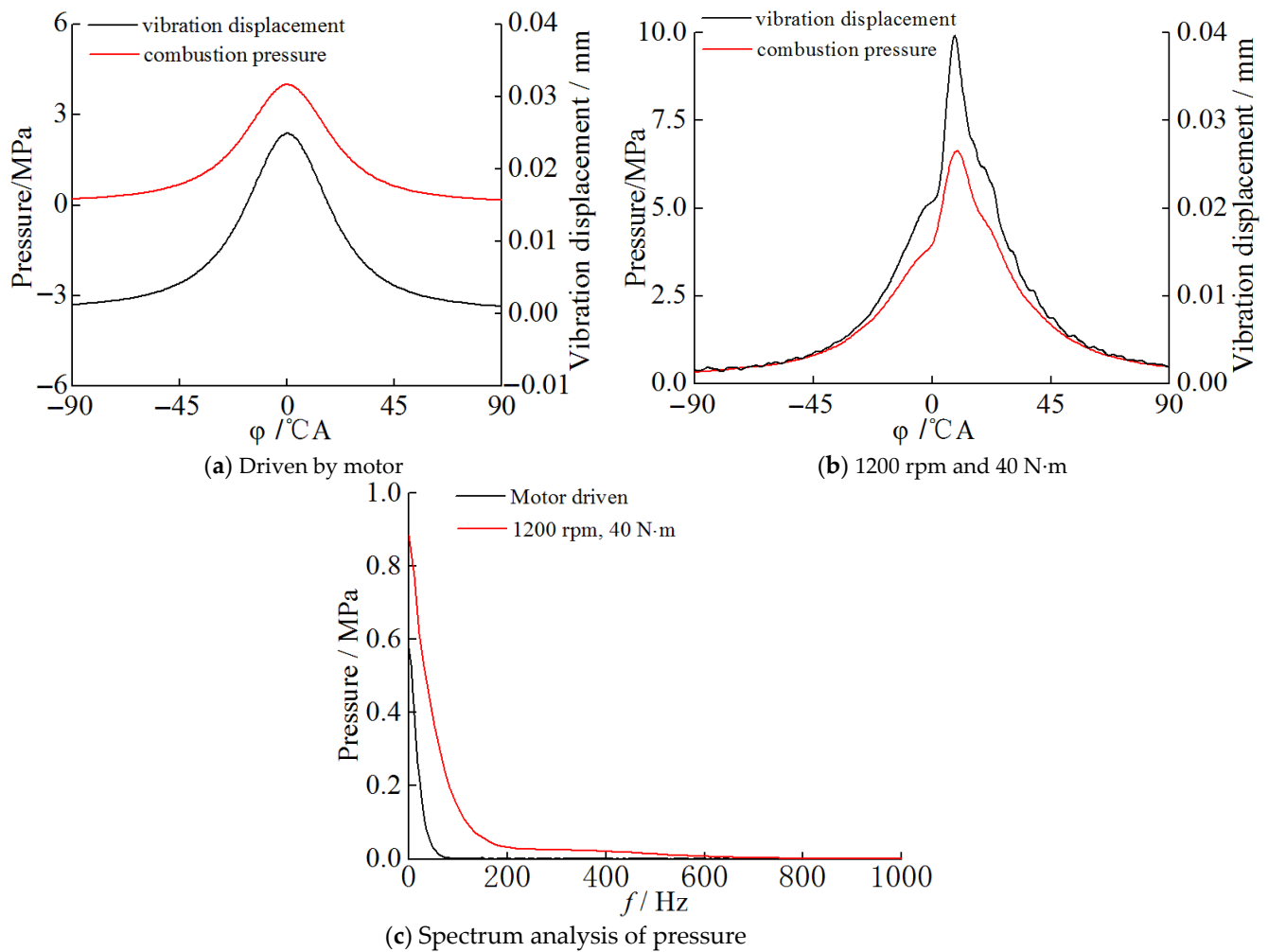


Figure 8. The time and frequency domain comparison under motor-driven and normal operating conditions.

According to the comparison, the relationship between the vibration and the combustion pressure can be divided into two stages. The two signals had the similar trend before the appearance timing of peak pressure, which can be considered as the first stage. After the appearance timing of peak pressure, the trend of the two signals had some differences, and this stage can be seen as the second stage. To further study the two-stage feature between the vibration displacement and the pressure during the normal operation, the vibration displacement was plotted against the pressure within 180° CA before and after the location of the peak pressure, as shown in Figure 9. It can be seen from Figure 9a that the relationship between the vibration displacement and pressure was almost linear before the SoC. This can be explained that the spectrum energy of pressure was lower than the first-order natural frequency due to the non-combustion state in this stage. After the SoC, the combustion pressure continued to increase until the peak pressure appeared, and the vibration displacement also presented a trend of increase. The combustion pressure and vibration displacement were an approximate linear relation, and the linear relationship was not as good as the signals before the SoC. The reason was that some high-frequency components around the natural frequency appeared due to the combustion; thus, the linear relationship between the two signals was influenced by the transfer characteristic of the engine. Owing to the smaller amplitude of these frequency components, the overall trend between combustion pressure and vibration displacement was approximately linear. The combustion pressure decreased after the peak pressure, and the vibration displacement fluctuated notably due to the action of the changing force and the transfer characteristic of the engine, which lead to the nonlinear relationship between the two signals, as seen in Figure 9b.

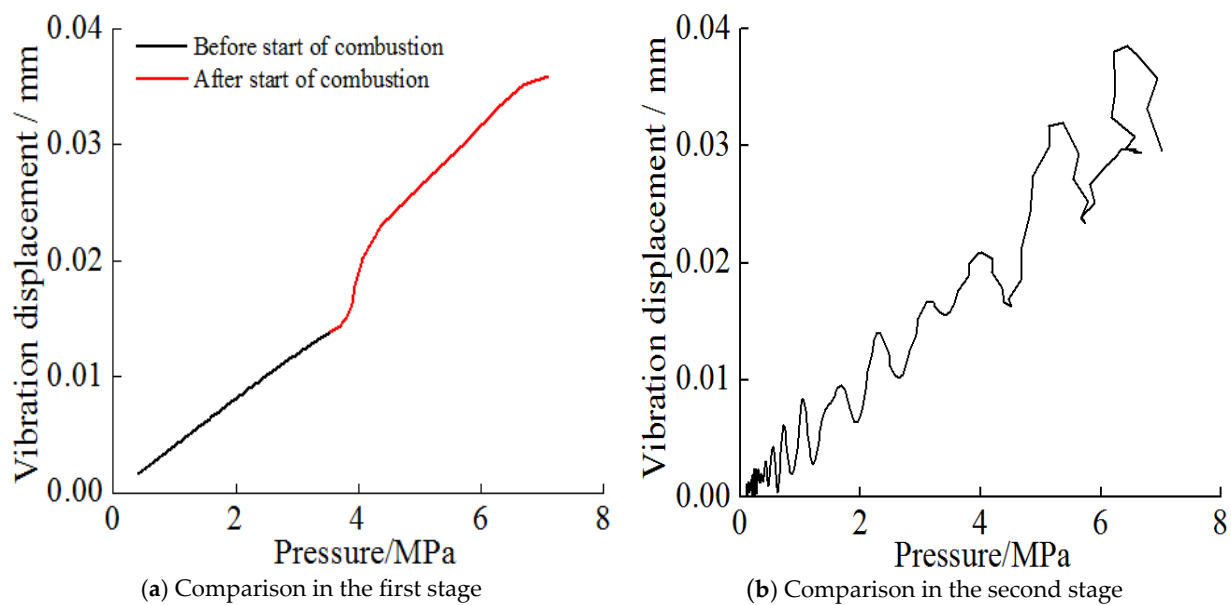


Figure 9. The two-stage relationship between combustion pressure and vibration displacement.

Based on the above analysis, it can be concluded that there existed an approximate linear relationship between pressure and vibration displacement before the appearance timing of peak pressure, especially before the SoC. The first and second derivative of vibration displacement were vibration velocity and acceleration, which should be linearly related to the first derivative of pressure (PIR) and the second derivative of pressure before the location of peak pressure. During this period, combustion status information can be estimated from the vibration signal. After the location of peak pressure, the vibration signal was inapplicable for combustion analysis due to the nonlinear relationship. The above finding can provide guidance for the proposal of fast processing method in the following sections.

3.2. Experimental Results

The combustion process of a diesel engine contains three stages: the first stage is called ignition delay period, in which fuel is injected and mixed with air in the combustion chamber; the second stage is called the rapid combustion period, in which the premixed mixture burns suddenly, and the quick increase of pressure leads to the notable vibration of the engine; the third stage is the diffusive combustion stage [19]. Measured vibration acceleration was compared with the PIR calculated from the measured combustion pressure at the load of 40 N·m and the speed of 1200 rpm, which is shown in Figure 10. The sudden increase point (φ_{ig} in Figure 10) of the PIR can be considered as the SoC [28]. Former analysis showed that vibration velocity was closely related to PIR, so vibration acceleration should correspond to the derivative of PIR. Therefore, the point of sudden increase of vibration acceleration (φ_{ig}' in Figure 10) was corresponding to φ_{ig} . The location of the peak PIR (φ_{pir} in Figure 10) was corresponding to the first downward zero-crossing point after φ_{ig}' , which is marked as φ_{pir}' in Figure 10. According to the corresponding relationship, the SoC and the location of peak PIR can be estimated according to the measured vibration acceleration.

There existed several excitations in an entire working cycle of the engine, such as combustion pressure, piston slap, and valve impact. Figure 11 shows the vibration acceleration and combustion pressure measured from the third cylinder. The amplitude of vibration acceleration achieved the highest value around the appearance timing of peak pressure. The estimated two combustion parameters were mainly located around the top dead center of compression stroke, and there still existed a time interval between the valve impact and the appearance timing of the two parameters for the studied twelve-cylinder engine. Therefore, the influence of valve impact can be eliminated from time domain.

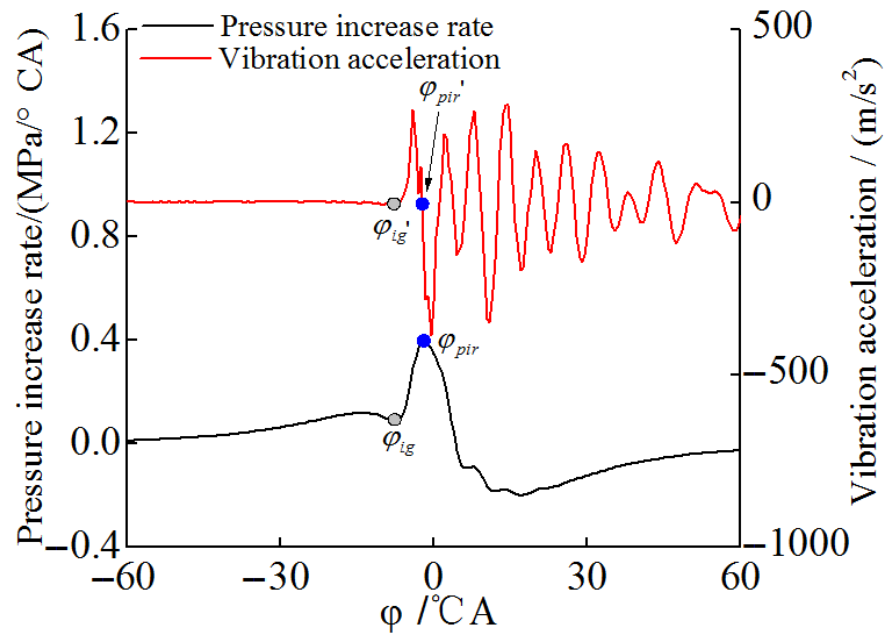


Figure 10. Comparison of PIR and vibration acceleration.

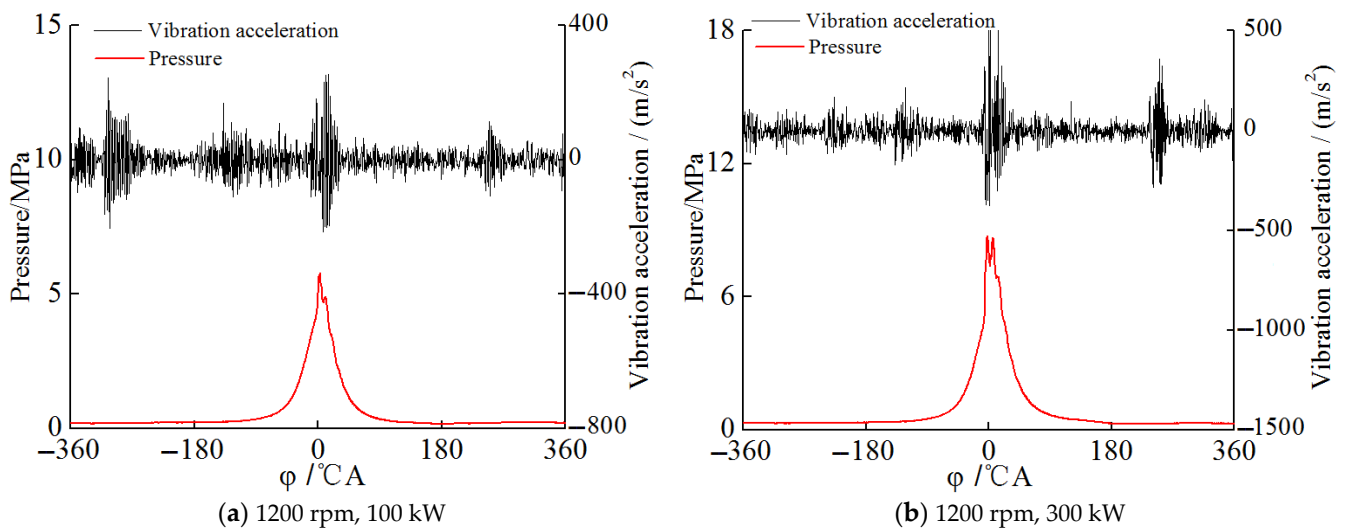


Figure 11. Vibration acceleration and pressure measured under different working condition.

The piston slap was another excitation source and overlapped with the combustion process; therefore, it is difficult to distinguish the two excitations in time domain. The characteristic of piston slap is an instantaneous process, and the spectrum of instant impact mainly consists of high-frequency components. Previous study showed that the frequency components of piston slap were mainly higher than 4000 Hz [28], and the frequency components of vibration signal related with combustion process was mainly lower than 1500 Hz [29–31]. The combustion pressure spectrum of the twelve-cylinder engine was calculated by FFT method, and the results are shown in Figure 12. The primary spectrum energy of the combustion pressure was lower than 2000 Hz for the twelve cylinders engine. Therefore, the combustion process and piston slap can be separated in frequency domain by a low-pass filter.

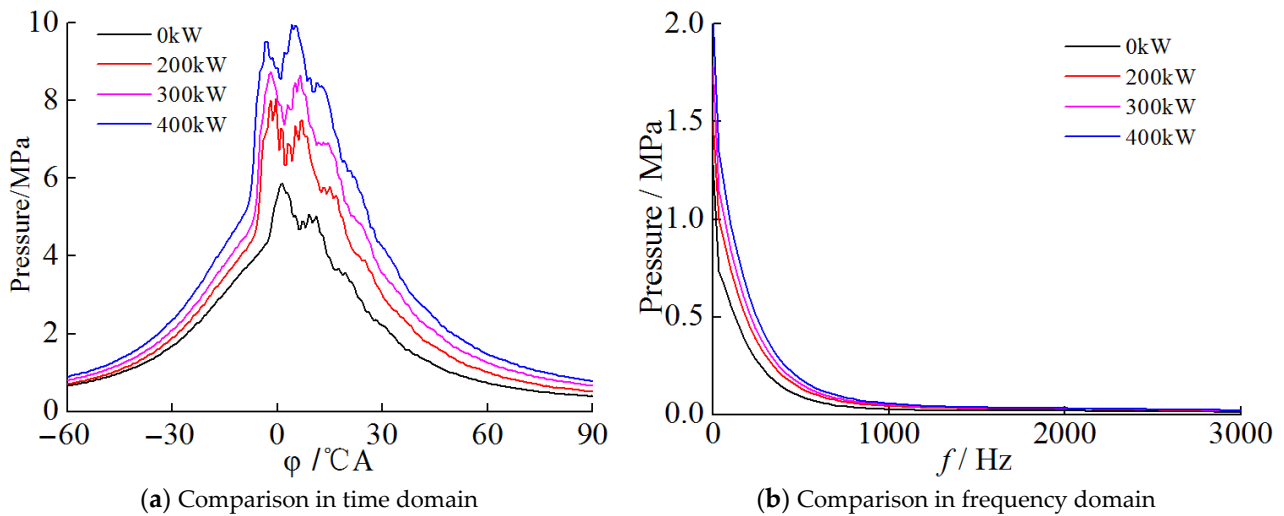


Figure 12. Time and frequency analysis of combustion pressure under the speed of 1200 rpm with different power.

Former analysis demonstrated that the low-frequency components of the vibration acceleration signal contained more combustion information. The measured vibration signal was filtered with a low-pass Chebyshev filter to retain the frequency components within 2000 Hz. The derivative of the PIR and the raw and filtered vibration signal were compared in Figure 13. The comparison showed that the raw vibration signal contained obvious high-frequency components, which can be eliminated with the low-pass filter. The trend of the filtered vibration acceleration signal was similar to the derivative of PIR. The correlation between the derivative of the PIR and filtered vibration acceleration in different working conditions was obvious, which proved the effectiveness of the former analysis.

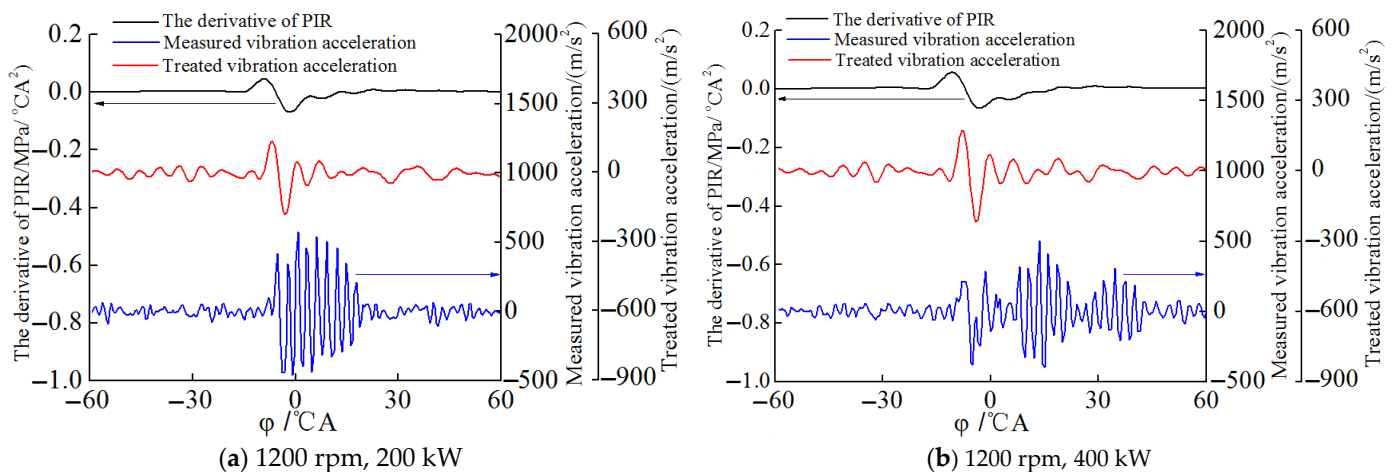


Figure 13. The comparison of the derivative of PIR and the raw and filtered vibration signal.

The precision of the proposed method was confirmed with the signals measured from the twelve-cylinder engine. The SoC and the appearance timing of the peak PIR were estimated with the feature points of vibration acceleration (φ_{ig}' and φ_{pir}' in the Figure 10). Figure 14 shows the comparison of the SoC from the vibration acceleration (φ_{ig}') and the PIR (φ_{ig}). It can be concluded that φ_{ig}' was, in general, later than φ_{ig} . An ICE can be considered as a test system in which the combustion pressure is an input, and the vibration signal is an output. The phase characteristic of the test system is influenced by the transfer characteristics of the engine. For the studied engine, the feature points of vibration acceleration were all delayed due to the transfer characteristics of the engine. According to the experiment data, the lag angle was basically unchanged in different

operation conditions, which can be considered as a system bias. Therefore, the lag angle can be calibrated in advance, and the estimated combustion parameters can be obtained from the vibration acceleration via the adjustment of the lag angle. Figure 14a shows the estimation deviation between φ_{ig} and φ_{ig}' was in the range of 4.7 to 7.3 °CA. The average value of the deviations was 6.48 °CA, and the value was used to adjust the estimated value of φ_{ig}' . After adjustment, most of the dispute was smaller than 1 °CA, and the maximum deviation was 1.48 °CA.

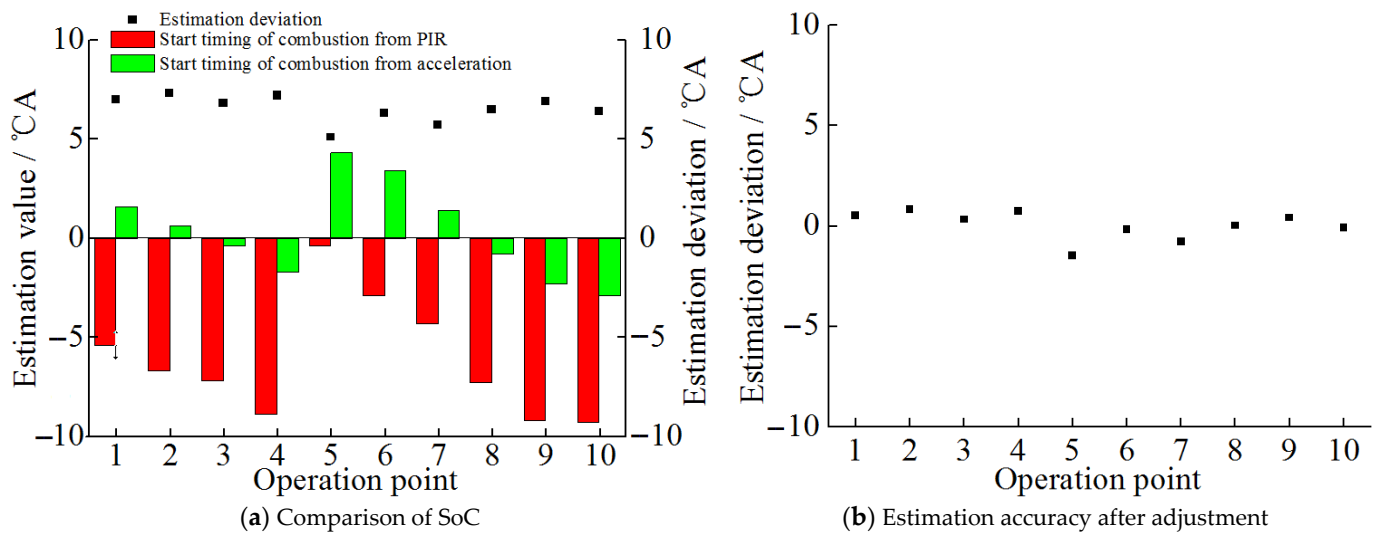


Figure 14. Accuracy comparison of SoC from PIR and acceleration. The operation points named 1 to 10 correspond to the engine operating condition showed in Table 3.

Similar analysis was conducted for the location estimation of peak PIR, and the comparison result is shown in Figure 15. For each operation point, the estimated timing of peak PIR (φ_{pir}') from the vibration acceleration was also later than the timing of φ_{pir} from PIR due to the transfer characteristics of the engine. The deviation range was from 0.3 to 1.2 °CA, and the average value of the deviations was 0.82 °CA. The average value was also used to adjust the values of φ_{pir}' . All the adjusted value of φ_{pir}' was smaller than 1 °CA. The accuracy is satisfactory and suggested that the proposed method can be used to extract the combustion information.

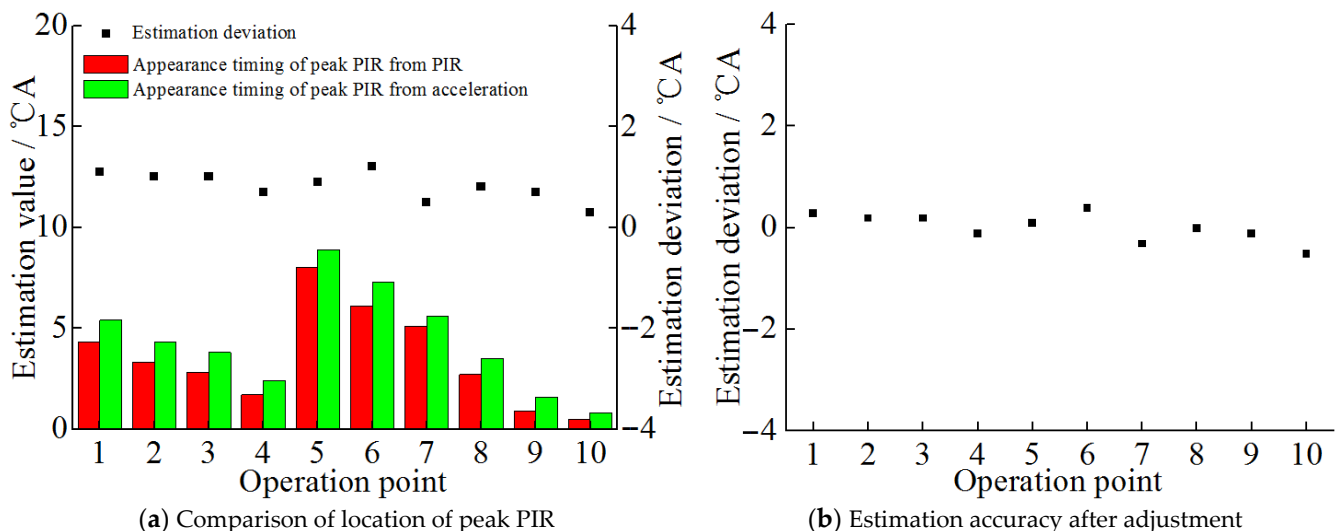
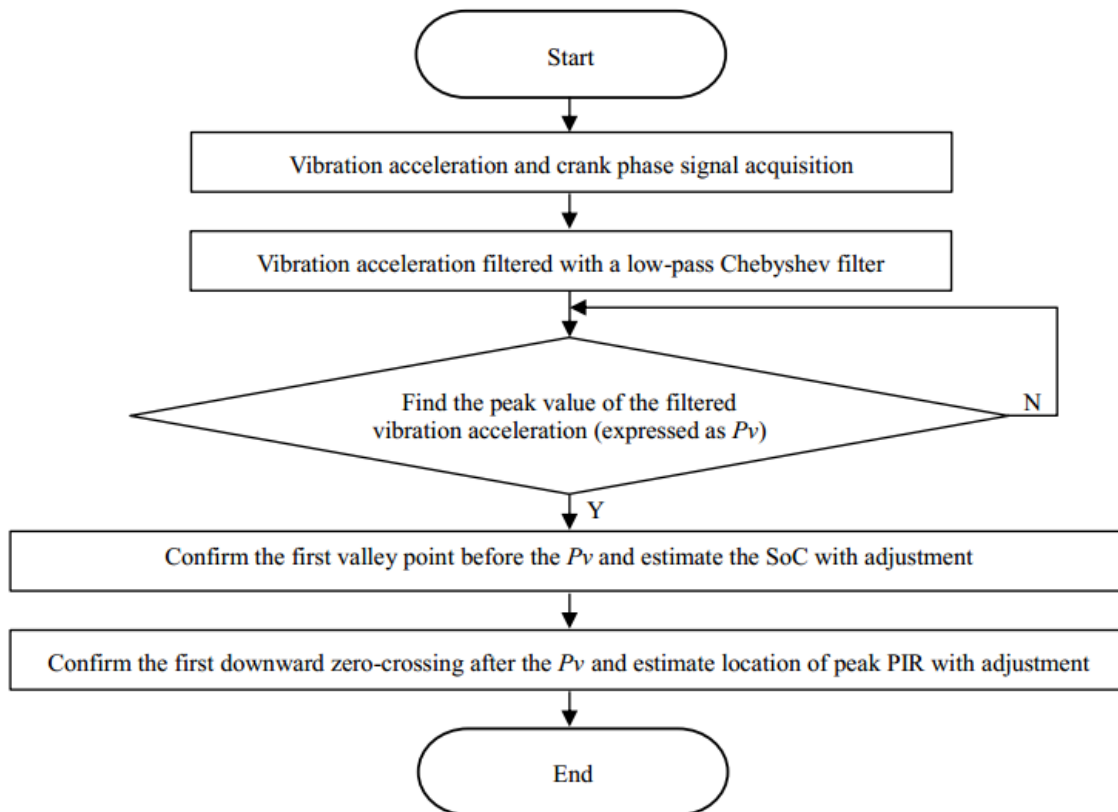
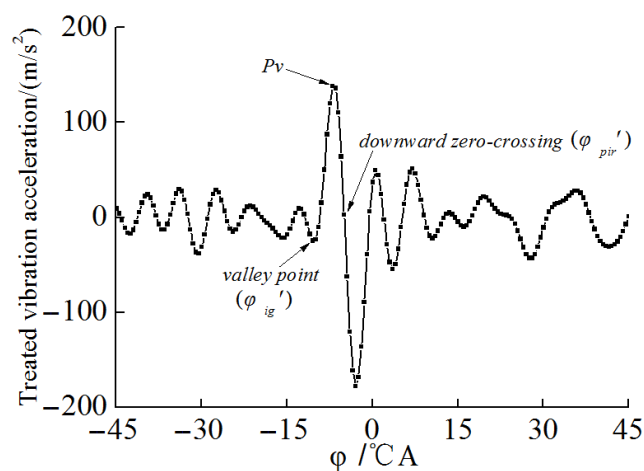


Figure 15. Accuracy comparison of location of peak PIR.

Based on the former analysis, a fast processing method was proposed to estimate the timings of SoC and the peak PIR. The data procession flow chart is shown in Figure 16a. The sampled vibration acceleration signal was firstly filtered with a low-pass Chebyshev filter. Then, the peak value of the filtered vibration acceleration (Pv) can be confirmed according to the crank phase signal, which can be seen in Figure 16b. The first valley point before the Pv and the first downward zero-crossing after the Pv can be used to estimate the appearance timing of SoC and the peak PIR with a system deviation correction. According to the former analysis in different working condition, the system deviation correction can be considered as the same for a giving engine, which can be obtained with a pre-calibration.



(a) The data procession flow chart of the fast processing method.



(b) The location of the key point

Figure 16. The data procession flow chart of the fast processing method and the location of the key points.

To verify the processing speed and accuracy of the proposed method, consecutive cycles of vibration signals were processed to obtain the crank angles of SoC and the peak PIR at the engine speed of 1500 rpm and the power of 450 kW. The estimation deviations of the two combustion parameters obtained from vibration acceleration and PIR are shown in Figure 17. Comparison results showed that the maximum deviation of the SoC and peak PIR were 1.98 and 1.25 °CA, respectively, at this working condition. Across the entire tested points, the maximum deviation of the SoC and peak PIR were below 2 and 1.5 °CA, respectively. The accuracy of the proposed method was therefore deemed adequate and acceptable. As the method only required simple calculations, which can be implemented by either hardware or software method, this proposed method can be considered feasible for closed-loop control systems.

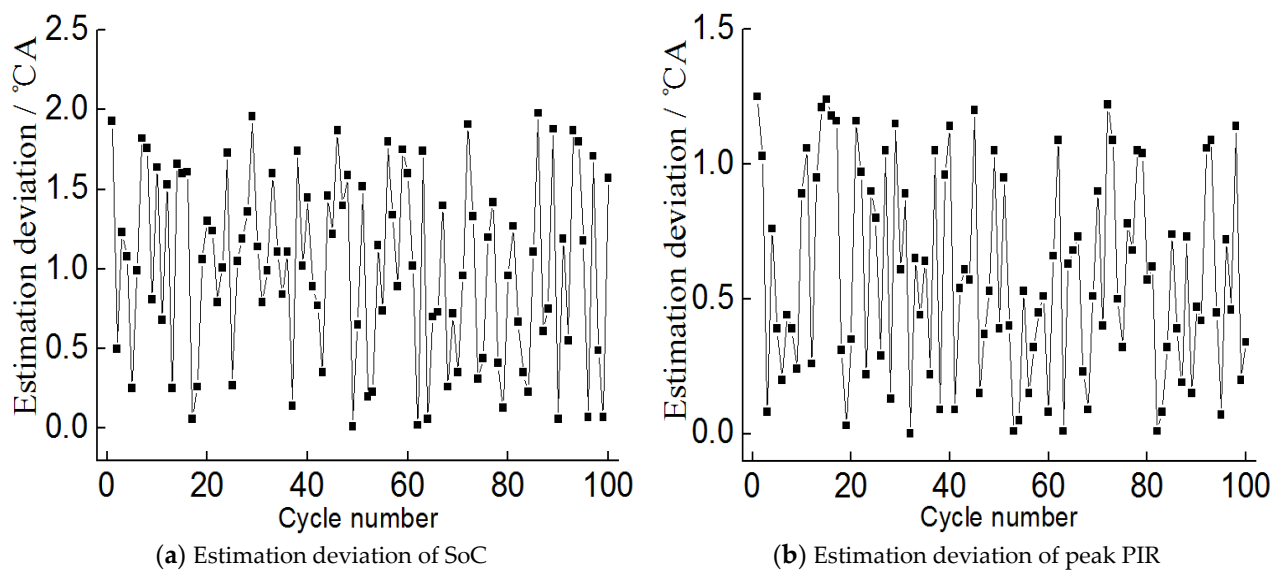


Figure 17. The estimation of SoC and peak PIR at the engine speed of 1500 rpm and the power of 450 kW.

4. Conclusions

A dynamic FEA model was developed with ABAQUS software and used to investigate the relationship between the combustion pressure and vibration response. The analysis confirmed the time correlation between the two signals. On this basis, a fast processing method was proposed to estimate the SoC and the appearance timing of the peak PIR. The proposed method was verified with a twelve-cylinder diesel engine. The main conclusions were shown as follows:

- (1) The relationship between the vibration displacement and the combustion pressure can be divided into two stages. The two signals had a similar trend before the timing of peak pressure. There existed an approximate linear relationship between the two signals before the timing of the peak pressure due to the major spectrum energy of pressure that was lower than the first-order natural frequency.
- (2) The vibration displacement fluctuated notably after the peak pressure due to the gradually decreasing combustion pressure and the transfer characteristic of the engine. The vibration signal in this period can hardly be used to estimate the combustion parameters owing to the small amount of useful information.
- (3) A fast processing method was developed to estimate the timing of SoC and peak PIR based on the low-pass filtered vibration acceleration. The two parameters were estimated from the sudden increase point and the first downward zero-crossing point, respectively. For the studied twelve-cylinder diesel engine, the maximum estimation deviation of the two combustion parameters were 2 and 1.5 °CA for the analysis of continuous cycles. The proposed method will be used to provide feedback signal for the closed-loop control of the combustion in the future research.

Author Contributions: Formal analysis, Y.L., X.L., and Y.C.; methodology, W.Y.; software, R.M.; validation, M.S.; visualization, S.Z.; writing—original draft, S.J.; writing—review and editing, G.T. All authors have read and agreed to the published version of the manuscript.

Funding: This study is financially supported by Shandong Key Research and Development Program, Shandong Province (Grant No. 2019GGX103042), Natural Science Foundation of Shandong Province (grant No. ZR2020ME180), State Key Laboratory of Engine Reliability, Weichai Holding Group Co., Ltd. (Grant No. WC0L-GH-2020-0191), National Natural Science Foundation of China (grant No. 51976107).

Institutional Review Board Statement: Not applicable.

Informed Consent Statement: Not applicable.

Conflicts of Interest: The authors declare no conflict of interest.

Abbreviations

Start of combustion (SoC); pressure increase rate (PIR); finite element method (FEM); crankshaft angle (CA); internal combustion engine (ICE); fast Fourier transform (FFT); Empirical Mode Decomposition (EMD); radial basis function (RBF); 50% mass fraction burned (MFB50); root-mean-square (RMS); heat release rate (HRR); intake valve open (IVO); intake valve close (IVC); exhaust valve open (EVO); exhaust valve close (EVC); before top dead center (BTDC); after bottom dead center (ABDC); before bottom dead center (BBDC); after top dead center (ATDC); multiple-degree-of-freedom (MDOF); torque (T_{iq}); speed (n); crank shaft angle (φ).

References

- Cheng, Y.; Tang, J.; Ji, S.; Huang, M. Combustion timing determination based on vibration velocity in HCCI engines. *Mech. Mach. Theory* **2012**, *58*, 20–28. [\[CrossRef\]](#)
- Ji, S.; Lan, X.; Lian, J.; Wang, H.; Li, M.; Cheng, Y.; Yin, W. Combustion parameter estimation for ICE from surface vibration using frequency spectrum analysis. *Meas. J. Int. Meas. Confed.* **2018**, *128*, 485–494. [\[CrossRef\]](#)
- Yang, W.; Yong, C. Vibration Measurement for Combustion Phase Evaluation in a CI Engine. *IFAC-Papers OnLine* **2018**, *51*, 821–826. [\[CrossRef\]](#)
- Hashim, M.A.; Nasef, M.H.; Kabeel, A.E.; Ghazaly, N.M. Combustion fault detection technique of spark ignition engine based on wavelet packet transform and artificial neural network. *Alex. Eng. J.* **2020**, *59*, 3687–3697. [\[CrossRef\]](#)
- Ji, S.; Cheng, Y.; Huang, W.; Huang, M. Comparison of the vibration sensors used in the estimation of the combustion process in a diesel engine. *Proc. IMechE Part D J. Automob. Eng.* **2014**, *228*, 863–872.
- Delvecchio, S.; Bonfiglio, P.; Pompoli, F. Vibro-acoustic condition monitoring of Internal Combustion Engines: A critical review of existing techniques. *Mech. Syst. Signal Process.* **2018**, *99*, 661–683. [\[CrossRef\]](#)
- Bi, F.; Ma, T.; Wang, X. Development of a novel knock characteristic detection method for gasoline engines based on wavelet-denoising and EMD decomposition. *Mech. Syst. Signal Process.* **2019**, *117*, 517–536. [\[CrossRef\]](#)
- Siano, D.; D’Agostino, D. Knock detection in SI engines by using the Discrete Wavelet Transform of the engine block vibrational signals. *Energy Procedia* **2015**, *81*, 673–688. [\[CrossRef\]](#)
- Taghizadeh-Alisaraei, A.; Ghobadian, B.; Tavakoli-Hashjin, T.; Mohtasebi, S.S.; Rezaei-asl, A.; Azadbakht, M. Characterization of engine’s combustion-vibration using diesel and biodiesel fuel blends by time-frequency methods: A case study. *Renew. Energy* **2016**, *95*, 422–432. [\[CrossRef\]](#)
- Sharma, A.; Sugumaran, V.; Devasenapati, S.B. Misfire detection in an IC engine using vibration signal and decision tree algorithms. *Meas. J. Int. Meas. Confed.* **2014**, *50*, 370–380. [\[CrossRef\]](#)
- Porteiro, J.; Collazo, J.; Patiño, D.; Míguez, J.L. Diesel engine condition monitoring using a multi-net neural network system with nonintrusive sensors. *Appl. Therm. Eng.* **2011**, *31*, 4097–4105. [\[CrossRef\]](#)
- Bizon, K.; Continillo, G.; Mancaruso, E.; Vaglieco, B.M. Towards on-line prediction of the in-cylinder pressure in diesel engines from engine vibration using artificial neural networks. *SAE Tech. Pap.* **2013**. [\[CrossRef\]](#)
- Johnsson, R. Cylinder pressure reconstruction based on complex radial basis function networks from vibration and speed signals. *Mech. Syst. Signal Process.* **2006**, *20*, 1923–1940. [\[CrossRef\]](#)
- Bizon, K.; Continillo, G.; Mancaruso, E.; Vaglieco, B.M. Reconstruction of in-cylinder pressure in a diesel engine from vibration signal using a RBF neural network model. *SAE Tech. Pap.* **2011**. [\[CrossRef\]](#)
- Ghamry, M.E.; Steel, J.A.; Reuben, R.L.; Fog, T.L. Indirect measurement of cylinder pressure from diesel engines using acoustic emission. *Mech. Syst. Signal Process.* **2005**, *19*, 751–765. [\[CrossRef\]](#)
- Omar, F.K.; Selim, M.Y.E.; Emam, S.A. Time and frequency analyses of dual-fuel engine block vibration. *Fuel* **2017**, *203*, 884–893. [\[CrossRef\]](#)

17. Scafati, F.T.; Lavorgna, M.; Mancaruso, E. Use of vibration signal for diagnosis and control of a four-cylinder diesel engine. *SAE Tech. Pap.* **2011**. [[CrossRef](#)]
18. Chiatti, G.; Chiavola, O.; Recco, E. Diesel combustion analysis via block vibration during engine transient operation. *SAE Tech. Pap.* **2013**. [[CrossRef](#)]
19. Carlucci, A.P.; Chiara, F.F.; Laforgia, D. Analysis of the relation between injection parameter variation and block vibration of an internal combustion diesel engine. *J. Sound Vib.* **2006**, *295*, 141–164. [[CrossRef](#)]
20. Morello, A.J.; Blough, J.R.; Naber, J.; Jia, L. Signal Processing Parameters for Estimation of the Diesel Engine Combustion Signature. *SAE Int. J. Passeng. Cars Mech. Syst.* **2011**, *4*, 1201–1215. [[CrossRef](#)]
21. Lee, S.; Lee, Y.; Lee, S.; Song, H.H.; Min, K.; Choi, H. Study on the Correlation between the Heat Release Rate and Vibrations from a Diesel Engine Block. *SAE Tech. Pap.* **2015**. [[CrossRef](#)]
22. Zhao, X.; Cheng, Y.; Ji, S. Combustion parameters identification and correction in diesel engine via vibration acceleration signal. *Appl. Acoust.* **2017**, *116*, 205–215. [[CrossRef](#)]
23. Zhao, X.; Cheng, Y.; Wang, L.; Ji, S. Real time identification of the internal combustion engine combustion parameters based on the vibration velocity signal. *J. Sound Vib.* **2017**, *390*, 205–217. [[CrossRef](#)]
24. Mao, J.; Hao, Z.Y.; Jing, G.X.; Zheng, X.; Liu, C. Sound quality improvement for a four-cylinder diesel engine by the block structure optimization. *Appl. Acoust.* **2013**, *74*, 150–159. [[CrossRef](#)]
25. Witek, L.; Zelek, P. Stress and failure analysis of the connecting rod of diesel engine. *Eng. Fail. Anal.* **2019**, *97*, 374–382. [[CrossRef](#)]
26. Metkar, R.M.; Sunnapwar, V.K.; Hiwase, S.D.; Anki, V.S.; Dumpa, M. Evaluation of FEM based fracture mechanics technique to estimate life of an automotive forged steel crankshaft of a single cylinder diesel engine. *Procedia Eng.* **2013**, *51*, 567–572. [[CrossRef](#)]
27. Ji, S.; Cheng, Y.; Huang, W.; Huang, M.; Huang, W.; Tang, J. Study on Relationship between cylinder head vibration displacement and cylinder pressure. *Chin. Intern. Combust. Engine Eng.* **2013**, *34*, 48–51.
28. Ji, S. On Description of Combustion Process Based on Vibration Acceleration Signal Measured from Cylinder Head. Ph.D. Thesis, University of Shandong, Jinan, China, 2008.
29. Arnone, L.; Boni, M.; Manelli, S.; Chiavola, O.; Conforto, S.; Recco, E. Diesel engine combustion monitoring through block vibration signal analysis. *SAE Tech. Pap.* **2009**. [[CrossRef](#)]
30. Chiavola, O.; Chiatti, G.; Arnone, L.; Manelli, S. Combustion characterization in diesel engine via block vibration analysis. *SAE Tech. Pap.* **2010**. [[CrossRef](#)]
31. Taglialatela-Scafati, F.; Cesario, N.; Lavorgna, M.; Mancaruso, E.; Vaglieco, B.M. Diagnosis and control of advanced diesel combustions using engine vibration signal. *SAE Tech. Pap.* **2011**. [[CrossRef](#)]